Optimising the Crystal Structure of a Novel 2D Metamaterial with Negative Statice Electric Susceptibility

Philip Wurzner
210930632
Dr. Flynn Castles
MSc Big Data Science

***Abstract*— In order to successfully create and experimentally test a 2D metamaterial which can levitate electric charges using its negative static electric susceptibility, the optimal meta-atom lattice geometry for the 2D material must be found. This study characterises the geometries of a metamaterial lattice in relation to the maximum polarisability its meta-atoms can take on before spontaneously polarising, and their density in the lattice, to find the optimal arrangement of meta-atoms for levitation purposes. The lattice was modelled using the Clausius-Mossotti model and the optimisation procedure was done using the Differential Evolution and Nelder-Mead methods. The optimal arrangement for the lattice was found to be a hexagonal lattice.**

Keywords—Optimisation, Metamaterials, Negative Electric Susceptibility, Machine Learning, Clausius-Mossotti

I. Introduction

Without the properties of differing types of wood, the Wright brothers would have been unable to take flight in 1903. Despite their humble origins, synthetic polymers, introduced to the world with invention of Bakelite in 1909, have facilitated countless pivotal modern industries and inventions. It is beyond reasonable doubt that the creation of novel materials properties is a key enabler of new technology and innovative engineering. Indeed, the European Commission estimates that 70% of all technical innovation is directly or indirectly predicated on advancements in materials properties [1]. Metamaterials stand at this frontier, creating unique functional properties that directly solve engineering problems. These intricately engineered materials are characterised by attributes which cannot be found in naturally occurring materials. While metamaterials particularly enjoy widespread use in electronic applications, they are by no means limited to this industry.

Certain metamaterials, such as the ones designed by Castles *et al*. [2], exhibit negative static electrical susceptibilities ($\mathcal{X}_e < 0$) which are traditionally asserted to be positive [3]. This property could offer an electric counterpart to negative magnetic susceptibilities, which provide means for diamagnetic levitation. Research into the use of diamagnetic levitation for applications such as sensing, actuators, and energy harvesting [4] is underway, and "dielectric levitation" could no doubt be considered for similar applications. Castles *et al*. achieve negative static electric susceptibility via the use of an active metamaterial. It consists of a lattice of "meta-atoms" which generate an artificial negative dipole in response to an applied field.

This paper builds on the work done by Dr Castles and Dutta at the School of Electronic Engineering and Computer Science in Queen Mary University of London. Using machine learning approaches, the meta-atom crystal structure of the metamaterial will be characterised and optimised to levitate a charged object, in the spirit of diamagnetic levitation. To achieve this aim, a 2D sheet of the metamaterial is modelled. To simulate the levitation characteristics, only the resulting dipole-moments normal to the sheet will be considered. This convention is referred to as a "2D-1D model".

II. Theoretical Background

A. Crystal Lattices

The repeating arrangements of atoms which can be found in crystalline materials such as metals are called lattices. In 2 dimensions, there are 5 types of lattices known as "Bravais lattices" [5]. Distinct systems have lattice arrangements which lend themselves to specific rules of symmetry. Despite this, most of the lattices can be described using the oblique lattice system. Lattices can either be described with magnitudes and an angle (a, b, θ), or primitive lattice vectors $(\mathbf{v}_1, \mathbf{v}_2)$. In a sense, the first lattice vector describes the relation between atoms in a row, and the second lattice vector could be seen as describing the relation between rows. These crystallographic conventions can also be used for the description of a metamaterial consisting of "meta-atoms" such as the ones developed by Castles *et al*.

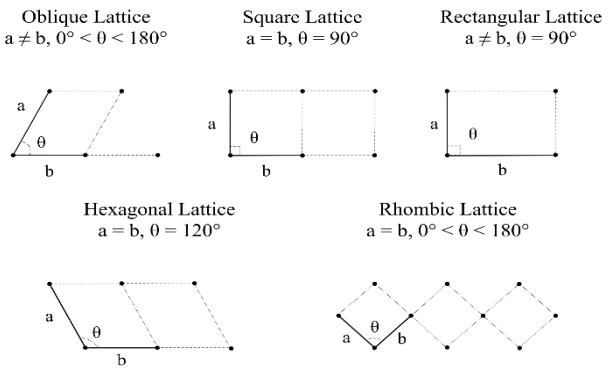

Figure 1 - Types of Bravais Lattices.

B. Electric susceptibility and polarisability

Atoms consist of a positive nucleus with a negatively charged cloud of electrons around it. In the presence of an electric field, the cloud of electrons distorts along the field. This phenomenon is known as polarisation and the separation of the positive and negative charges is characterised as an induced dipole moment[6]. In non-polarised systems, atoms do not have permanent dipole moments, and such systems only form dipole moments under an externally applied electric field. For certain systems with low electric susceptibilities $\mathcal{X}_e$, no external field is needed for permanent dipoles to form between atoms and the material to polarise. This is commonly referred to as "spontaneous polarisation" and these materials are referred to as ferroelectric [7]. This polarisation could be reverted using external electric fields.

On a macroscopic scale, the relationship between a system's electric susceptibility $\mathcal{X}_e$, the electric field applied to the system **E,** and polarisation density **P** is as follows

$$\mathbf{P} = \mathcal{X}_e \mathbf{E} \varepsilon_0, \tag{2.1}$$

where ε_0 is a constant known as the permittivity of free space. On a microscopic scale, the polarisability α (i.e. a point's tendency to polarise) of a system is used to calculate the dipole moment $\boldsymbol{\mu}$ of each point in the system [6], [8].

$$\boldsymbol{\mu} = \alpha \mathbf{E} \tag{2.2}$$

The Clausius-Mossotti relation (CM), based on charge distribution fields and the volumes occupied by atoms, allows us to establish a link between the macroscopic and microscopic views of (2.1) and (2.2) using the density of polarisable points in the system n [5], [9].

$$\boldsymbol{\mathcal{X}}_e = \frac{\frac{n\alpha}{\varepsilon_0}}{1 - \frac{n\alpha}{3\varepsilon_0}} \tag{2.3}$$

It is generally held that electric susceptibilities are not negative in naturally occurring systems [3]. Despite this, the CM does not require the polarisability of point charges to be positive to effectively describe an electric arrangement. Theoretically, a system with a negative electric susceptibility would see its point charges polarise in the opposite direction to an applied field as is observed for negative magnetic susceptibilities. This effect would result in a repulsion between the material and the source of the external field. The magnetic analogue of this, diamagnetism, has been used to great effect to levitate objects such as frogs [10].

C. The Generalised Clausius-Mossotti Model of Spontaneous Polarisation

The Clausius-Mossotti model (CMM), as used by Allen [11], [12], facilitates a classical approach to simulating whether a lattice of atoms spontaneously polarises, depending on factors such as the polarisabilities of the atoms, the geometry of the lattice, and the strength of an external field. Two key assumptions are made in the use of this model, namely that all atoms in the lattice are fixed and all atoms must share the same polarisabilities.

With these assumptions, in a lattice of atoms with a polarisability of α, the electric dipole moment $\boldsymbol{\mu}_i$ generated by each atom is:

$$\boldsymbol{\mu}_i = \alpha \mathbf{E}_{\text{tot}} \tag{2.4}$$

Where $\mathbf{E}_{\text{tot}}$ is the total electric field which is present at the atom i. This total field can be defined as the sum between an external field $\mathbf{E}_{\text{ext}}$ and induced field $\mathbf{E}_{\text{ind}}$. The sum of all dipole moment fields at point i, which come from the other atoms j, is the induced field $\mathbf{E}_{\text{ind}}$ [5], [12].

$$\mathbf{E}_{\text{ind}} = \sum_j^{\neq i} \frac{3\mathbf{R}_{ij}\left(\mathbf{R}_{ij} \cdot \boldsymbol{\mu}_j\right) - \left|\mathbf{R}_{ij}\right|^2 \boldsymbol{\mu}_j}{4\pi\varepsilon_o \left|\mathbf{R}_{ij}\right|^5} \tag{2.5}$$

Where $\mathbf{R}_{ij}$ is the vector between i and j, $\boldsymbol{\mu}_j$ is the electric dipole moment of j, and $\left|\mathbf{R}_{ij}\right|^2$ is the magnitude of the vector between the two atoms. Following this, the distances between atoms can be normalised by dividing the distance term by the magnitude of one of the lattice vectors, arbitrarily chosen to be $\mathbf{v}1$, ensuring its length will always be 1, as seen on Fig. 2.

$$\mathbf{v}1 = \begin{bmatrix} a \\ 0 \end{bmatrix} \tag{2.6}$$

$$\mathbf{R}'_{ij} = \frac{\mathbf{R}_{ij}}{|\mathbf{v}1|} = \frac{\mathbf{R}_{ij}}{v1} = \frac{\mathbf{R}_{ij}}{a} \tag{2.7}$$

$$\mathrm{E}_{\text{ind}} = \sum_j^{\neq i} \frac{3\mathbf{R}'_{ij}\left(\mathbf{R}'_{ij} \cdot \boldsymbol{\mu}_j\right) - \left|\mathbf{R}'_{ij}\right|^2 \boldsymbol{\mu_j}}{4\pi\varepsilon_o |\mathbf{v}1|^3 \left|\mathbf{R}'_{ij}\right|^5} \tag{2.8}$$

Substituting (2.8) into (2.2),

$$\boldsymbol{\mu}_i = \alpha \left(\mathbf{E}_{\text{ext}} + \sum_j^{\neq i} \frac{3\mathbf{R}'_{ij}\left(\mathbf{R}'_{ij} \cdot \boldsymbol{\mu}_j\right) - \left|\mathbf{R}'_{ij}\right|^2 \boldsymbol{\mu_j}}{4\pi\varepsilon_o |\mathbf{v}1|^3 \left|\mathbf{R}'_{ij}\right|^5} \right). \tag{2.9}$$

This expression can be simplified using key facts of the simulation. Firstly, since spontaneous polarisability is of interest, $\mathbf{E}_{\text{ext}} = 0$, and secondly, we can combine the constants in the denominator of 2.8 together with α to create a new variable $\alpha'$and additionally simplify the equation.

$$\alpha' = \frac{\alpha}{4\pi\varepsilon_o |\mathbf{v}1|^3} \tag{2.10}$$

$$\boldsymbol{\mu}_i = \alpha' \left(\sum_j^{\neq i} \frac{3\mathbf{R}'_{ij}\left(\mathbf{R}'_{ij} \cdot \boldsymbol{\mu}_j\right) - \left|\mathbf{R}'_{ij}\right|^2 \boldsymbol{\mu_j}}{\left|\mathbf{R}'_{ij}\right|^5} \right) \tag{2.11}$$

Further, we are only considering the resulting field normal to the 2D material ($\mathbf{R_{ij}} \perp \boldsymbol{\mu}_j$) for levitation purposes, $\mathbf{R}_{ij} \cdot \boldsymbol{\mu}_j = 0$. This gives us:

$$\boldsymbol{\mu}_{\text{i}} = \alpha' \left(\sum_j^{\neq i} -\left|\mathbf{R}'_{ij}\right|^{-3} \boldsymbol{\mu}_j \right). \tag{2.12}$$

One can also express (2.12) in a matrix form, as shown below, where $\mathbf{R}_n$ consists of the magnitude distance term $\left|\mathbf{R}_{ij}\right|^{-3}$.

$$\boldsymbol{\mu} = \alpha' \mathbf{R}'_{\boldsymbol{n}} \boldsymbol{\mu} \tag{2.13}$$

The resulting distance matrix ($\mathbf{R}'_n$) is a real and symmetric. (2.13) can then be rearranged into a eigenvalue equation with the identity matrix **I**:

$$\left(\frac{1}{\alpha'}\mathbf{I} - \mathbf{R}'_n\right)\boldsymbol{\mu} = 0. \tag{2.14}$$

In the case that all eigenvalues of $\frac{1}{\alpha}\mathbf{I} - \mathbf{R}_n$ positive, the system of meta-atoms is stable. This is due to the minimisation of an enery function $f(\boldsymbol{\mu}_i)$ which occurs for the solution for the dipoles.

$$f(\boldsymbol{\mu}_i) = \frac{1}{2\alpha'} \boldsymbol{\mu}^{\top} \left(\frac{1}{\alpha'}\mathbf{I} - \mathbf{R}'_n\right) \boldsymbol{\mu} \tag{2.15}$$

Since $\mathbf{R}_n$ is a real, symmetric, and traceless matrix it must feature at least one positive and one negative eigenvalue. When taking the inverse extremes of these eigenvalues ($\alpha'_{c+} = \frac{1}{\lambda_{\max}}$, $\alpha'_{c-} = \frac{1}{\lambda_{\min}}$) one can find the bounds of α' for which the system maintains stability, and does not spontaneously polarise. These critical polarisabilities therefore give the maximum possible values of α' the system can take before it becomes unstable. For a fixed distance $|\mathbf{v}1|$ the maximum α can be determined using equation (2.10).

III. Literature Review

A. Metamaterials

Metamaterials (MMs) allow for the design of novel and exotic materials properties. Generally, these materials obtain their features from artificially engineered structures, rather than their chemical composition [13]. A subset of MMs are known as "Active", and such MMs use an external power supply which enables them to display an exceptional range of properties. Pivotally, active MMs are known to be capable for a wider array of interesting properties than passive MMs [14], [15].

Surprisingly, the first use of an MM dates back as far as 1898, when Prof. Bose [16] proposed a novel method of polarising microwave electric fields using an MM, but the MM concept hadn't been formalised until 1967, by Prof. Veselago [17], who theorised the existence of "left-handed substances". A lull in research on the topic followed this, until Prof. Pendry *et al*. revitalised interest with his demonstration of a material with negative permittivity in 1996 [18] and permeability in 1999 [19]. Since then, the scope of metamaterials has broadened, and work on metamaterials has not slowed down – evidenced by the rate at which papers on the subject are produced, which has been consistently increasing since 2010.

Modern MMs often mimic atomic structures, with each "meta-atom" displaying purpose-chosen characteristics. Examples of modern MMs include those with negative Poisson ratios [20], negative refractive indexes [21], and inverse Doppler effects [22]. More recently, MMs with enhanced vibration isolation [23], perfect wave absorption [24], and water purification [25]capabilities have been developed. These exciting properties may be used to further improve or enable novel technologies.

B. Negative Static Electric Susceptibility

In key works on electrodynamics, such as the work by Landau *et al*. [26], it is stated that static electric susceptibilities must be positive for all materials. This belief is further supported by more recent papers, such as Wood and Pendry [27], which theorise this must also be true for MMs. Despite this, it has been noted by Sanders [3] and Chiao *et al*. [28]–[31] that this principle may not necessarily be inviolable for materials which are not in thermodynamic equilibrium. Indeed, both Sanders and Chiao have reasonably predicted the feasibility of such materials, but never experimentally verified their theories.

Now nascent research is being done on developing MMs which exhibit the theorised negative static electric susceptibilities, such as the work done by Castles *et al*. [2]. Castles *et al*. designed and experimentally tested the effectiveness of 2 metamaterials with negative electric susceptibilities. These materials feature a meta-atom structure and polarise in the opposite direction when an external field is applied. Each meta-atom is designed to detect a magnetic field and generate an artificial dipole in the desired opposite direction and do so in proportion to the strength of the externally applied field. Despite success in providing a proof of concept, the MM must be further improved upon to be able to "dielectrically" levitate objects.

C. Machine Learning and Optimisation

Machine learning approaches in science and engineering have become increasingly popular due to the success of algorithms such as DeepMind's AlphaFold [32] and federal initiatives such as the US' "Materials Genomics Initiative" [33] and the EU's "Horizon Europe" [34]. A key component of machine learning are optimisation algorithms, which seek to minimise variables within a given parameter space.

Generally, optimisation algorithms seek to solve the following problem statement [35]:

$$\begin{aligned} &\text{minimise} \quad f(\mathbf{x}) \\ &\text{subject to} \quad \mathbf{x} \in \Omega \end{aligned} \tag{3.1}$$

The function f is a real-valued function known as the objective function (OF). Its parameters $\mathbf{x}$, known as its decision variables (DVs), is a vector of size n. If these parameters are limited in the values they can take on, the optimisation is said to be bound.

$$f : \mathbb{R}^n \to \mathbb{R} \tag{3.2}$$

$$\mathbf{x} = [x_1, x_2, \dots, x_n]^\top \in \mathbb{R}^n \tag{3.3}$$

If the certain combinations of DVs are not feasible this can be represented with Ω. Ω is the subset of $\mathbb{R}^n$ in which the optimisation algorithm searches for minima. This is known as the constraint set, with can be defined a constraint function.

Many optimisation algorithm paradigms exist, each designed to solve particular styles of problems. An important distinction must be made between local and global optimisation routines. Local optimisation procedures generally seek to find the first local minimum they can find and terminate. Global optimisation procedures, on the other hand, thoroughly characterise the parameter space and seek a global minimum before terminating [36]. This widened scope makes global optimisation algorithms more practical for many scientific applications, at the cost of longer runtimes, a higher chance of not converging, and more complex operations.

Another way optimisation algorithms are classified is whether they require derivatives of the OF. Algorithms which do not rely on derivates are referred to as "black-box", "direct" or "zero-order". Depending on how the objective function is obtained, the data can be noisy or inconsistent. OFs with these characteristics are generally unsuited for derivative-based optimisation routines and it is preferred to use black-box algorithms instead [37]. A subclass of black-box algorithms use stochastic methods (SMs). SMs use randomisation to preform the search of the variable space. A derivation of stochastic models are population methods (PMs). PMs randomly generate "individuals" across the

parameter space which work together to find a global minimum. This contrasts with usual optimisation approaches, which tend to incrementally move a single point to find a minimum.

The "Nelder-Mead Simplex" method [37], [38] is a local black-box optimisation algorithm, capable of using bound DVs and a constraint function, which works by constructing simplexes, which take on the shape of a triangle in 2D, in the variable space. It was developed in 1965 by Nelder and Mead. The coordinates of the simplex are adjusted based on the values of the OF at the vertices of the simples. As the algorithm iterates on the simplex, it reduces in size until it eventually converges on the local minimum. Every iteration of updating the simplex evaluates 4 operations: reflection, expansion, contraction, and shrinkage. The operation which brings the simplex closer to a local minimum is performed and the next iteration begins.

The "Differential Evolution" method is a global black-box optimisation algorithm using the population method designed by Storn and Price in 1997 [37], [39]. It works by generating individuals over the variable space and then combining individuals in accordance with a weighted formula, which can typically be characterised as needed. If a combination of individuals leads to an improved OF evaluation it is accepted, and if not, it is rejected. This combination procedure is done in iterations until the individuals have converged on the global minimum or settled in local minima. While this method can search a large variable space, and deal well with noisy functions, it generally requires a higher amount of OF evaluations. For this reason, it is not used in cases where the OF is computationally expensive.

Equally as important as the selection of the algorithm is the setting of the hyperparameters driving the optimisation. Careful consideration must be given to the number of iterations, population sizes, and convergence tolerances for the optimisation procedure to be successful and completed in a timely manner.

IV. Methodology

A. Definitions and Objective Function

The closer two meta-atoms are to each other in a lattice, the lower the polarisability of each atom must be to prevent spontaneous polarisation. On the other hand, the more densely packed the atoms are, the greater the strength of the field is for a given polarisability. Assuming that any polarisability can be chosen for Castles *et al*'s MM, an optimal compromise between the density of the meta-atoms and the corresponding critical polarizability α_{c-} of the system can be made.

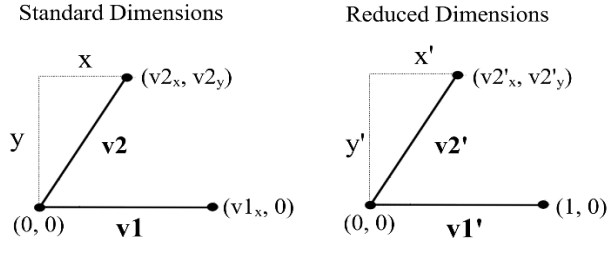

Figure 2 – Variables defining the meta-atom lattice.

The geometry of the meta-atom lattice is described using lattice vectors, as shown in Fig. 2. The first vector has arbitrarily been limited along the x-axis, to prevent equivalent lattices from forming at differing angles.

$$|\mathbf{v}1| = v1_{\mathrm{x}} \tag{4.1}$$

Furthermore, the dimensions of the lattice can be reduced by dividing $\mathbf{v}1$ and $\mathbf{v}2$ by the magnitude of $\mathbf{v}1$. This normalises the length of $\mathbf{v}1$ to 1 and removes the equal lattices $(\mathbf{v}1, \mathbf{v}2) = (\mathbf{v}2, \mathbf{v}1)$, creating the lattice vector $\mathbf{v}2'$

$$\mathbf{v}2' = \frac{\mathbf{v}2}{v1_{\mathrm{x}}} \tag{4.2}$$

To find the optimal point density for the meta-atom structure, the objective function (OF) must be defined in terms of the lattice vectors $\mathbf{v}1, \mathbf{v}2$. In this instance, the OF n, represents the density of polarisable points as used in (2.3), which can be defined as:

$$n = \frac{1}{\text{area of unit cell}} \tag{4.3}$$

$$n = \frac{1}{(v1_x)(v2_y)} \tag{4.4}$$

Where $v1_x$ and $v2_y$ are the x and y components of their respective vectors. Using the definitions of the normalised lattice, as shown in Fig. 2,

$$v2'_y = \frac{v2_y}{v1_x} \tag{4.5}$$

$$N = \frac{1}{\mathrm{v}2'_y(\mathrm{v}1_x)^2} \tag{4.6}$$

Rearranging (2.10) and recalling (4.1),

$$|\mathbf{v}1| = v1_x = \left(\frac{\alpha}{4\pi\varepsilon_o\alpha'}\right)^{\frac{1}{3}} \tag{4.7}$$

Substituting (4.7) into (4.6),

$$n = \frac{1}{v2'_y\left(\frac{\alpha}{4\pi\varepsilon_o\alpha'}\right)^{\frac{2}{3}}} \tag{4.8}$$

$$\frac{n}{\left(\frac{4\pi\varepsilon_o}{\alpha}\right)^{\frac{2}{3}}} = \frac{1}{v2'_y\left(\frac{1}{\alpha'}\right)^{\frac{2}{3}}} \tag{4.9}$$

$$\frac{n}{\left(\frac{4\pi\varepsilon_o}{\alpha}\right)^{\frac{2}{3}}} = \frac{(\alpha')^{\frac{2}{3}}}{v2'_y} \tag{4.10}$$

Given that the denominator on the left-hand side is a constant, n may be simplified to n'. Moreover, to signify that only the negative α_c is of interest, where the lattice spontaneously polarises, α' and n'_c are set as α'_{c-} and n'_{c-}.

$$n'_{c-} = \frac{(\alpha'_{c-})^{\frac{2}{3}}}{v2'_y} \tag{4.11}$$

This leaves us the OF, defined by the critical polarisability α'_{c-}, found with the smallest eigenvalue of $1/\mathbf{R}'_n$, and the magnitude of the reduced y-component of the second lattice vector $\mathbf{v}2'$.

B. Development and characterisation of the $\mathbf{R}'_n$ simulation

The 2 pivotal aspects of a good OF for preforming successful optimisations are low runtimes and low error. Significant efforts were made to ensure these characteristics of the simulation were adequate before proceeding with the optimisation procedure.

The 3-dimensional version of the dipole-dipole relation script, first developed by Dutta using MATLAB®, calculates the $\mathbf{R}'_n$ with nestled loops to fill out a matrix of size $3N \times 3N$. Using the simplifications unique to the 2D-1D case, as outlined in II.C, the looping operation was vectorised to matrix operations on a matrix of size $N \times N$ in Python. Secondly, the manner in which the lattice coordinates were generated was also sped up. Rather than generating every point with 2 nestled loops, the simulation now generates rows of points, of size N, using the $\mathbf{v}1'$. Following this, the program generates the next row but displaced from the first row by $\mathbf{v}2'$. This creates a slanted matrix in a computationally efficient manner. Finally, a "just-in-time" (JIT) python compiler, numba [40], was used to further speed up segments of the code. These optimisations resulted in a runtime improvement of ~700% at simulation sizes of 100×100 meta-atoms. It should be noted, however, that these runtime improvements have come at the cost of memory usage, and therefore the feasible range of simulation sizes N is smaller than the previous model. Given that optimisation procedures require high speed simulations, it was felt that this was a necessary compromise.

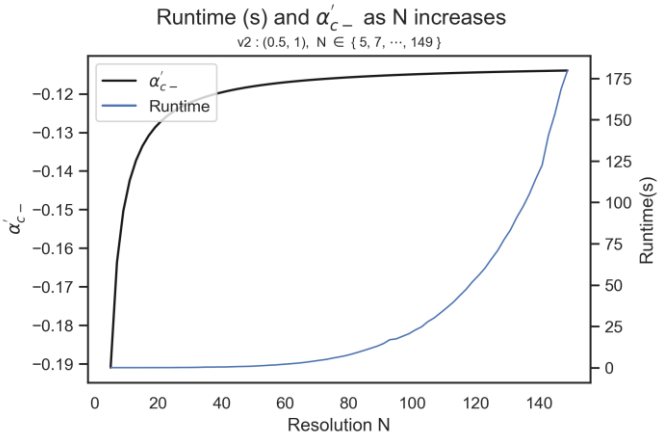

Figure 3 - Runtime and α'_{c-} with simulation size N.

Each simulation is run with a lattice of size N. The error of the simulation is largely dependent on N, since a perfect simulation would represent a lattice of infinite size $N = \infty$. Given that simulating an infinite lattice is impossible using our methods, two simulations of finite N can be extrapolated to $\frac{1}{N} = 0$ as an alternative. To establish the error margin in inherent to this approach, simulations of a range of N were done, using arbitrary $\mathbf{v}2'$. In doing so, the extrapolations of low-resolution simulations can be directly compared to those of high resolutions, as shown in Fig. 4-6. The linear extrapolations of the two lowest resolutions (5,7) can be seen to predict much lower $|\alpha'_{c-}|$ than the highest resolution simulations (121, 123).

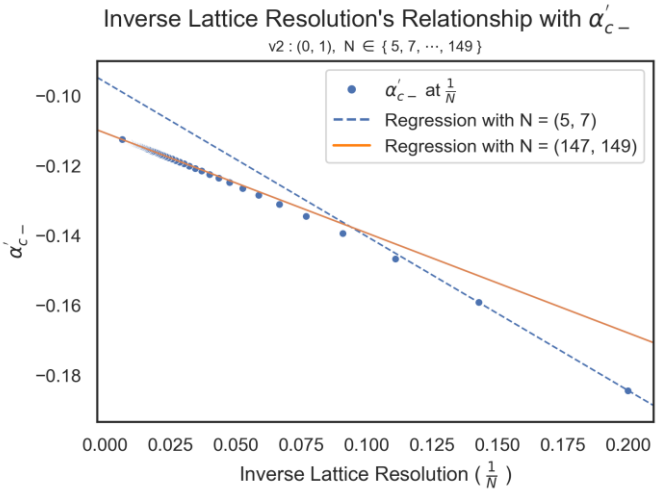

Figure 4 - Extrapolations to $N = \infty$ using $\boldsymbol{v}2' = (0,1)$.

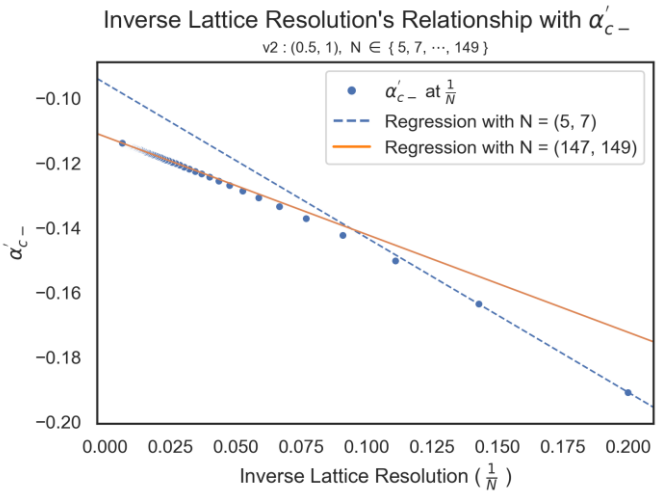

Figure 5 - Extrapolations to $N = \infty$ using $\boldsymbol{v}2' = (0.5, 1)$.

Using this method and $\mathbf{v}1'$ values of $(0,1)$ and $(0.5, 1)$, a relative average error can be selected as a function of N and $N - 2$. Setting the highest acceptable error to 1%, the resolutions of $N = (19, 21)$ were chosen to extrapolate to $N = \infty$. These specifically give an estimated relative error of $\sim 0.9\%$ with an approximate runtime of 86 ms per simulation cycle.

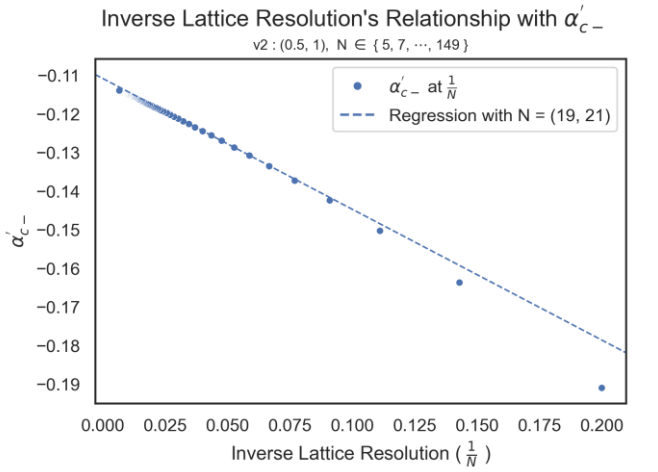

Figure 6 – Selected regression to extrapolate to $N = \infty$.

C. Optimisation Hyperparameters

To perform a succinct optimisation, the variable space of the lattice was bound in several regards. First, $\mathbf{v}1$ was set to (1,0), as shown in Fig. 2. As a result of the normalisation of distances using $\mathbf{v}1$, its magnitude must be 1. The normalisation of distances removes the need run simulate at a wide range of scales, and constricts the symmetry of possible lattices, since lattices defined by $(\mathbf{v}1, \mathbf{v}2) = (\mathbf{v}2, \mathbf{v}1)$. The other lattice vector $\mathbf{v}2$ has been limited on the x-plane to never exceed 0.5, since there exists a symmetry between $0 \leq v2_x < 0.5$ and $0.5 < v2_x < 1$. Preliminary modelling, as shown in Fig 7, reveals a periodicity wherein $f(x) = f(1-x)$ within $0 \leq x \leq 1$.

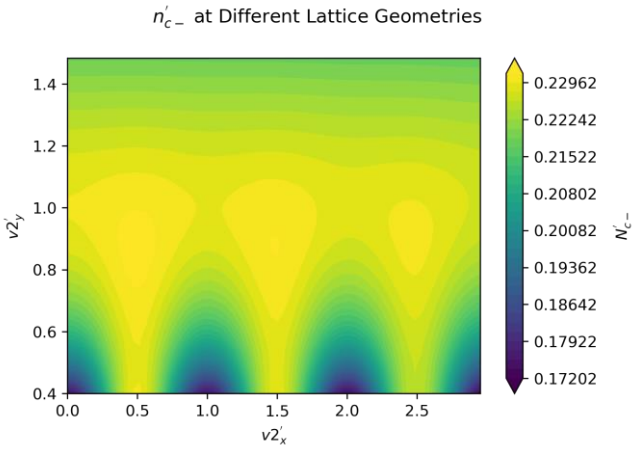

Figure 7 –Contour Plot of Values of n'_{c-} at Various Lattice Geometries with v2' = ($v2'_x$, $v2'_y$).

Beyond $x > 1$ the lattice distorts, as shown in Fig. 8, slanting further due to the placement of the atoms on the layer above. This causes some degree of error which can be spotted on the contour plot, but the simulation maintains the general relationships as previous $v2_x$ cohorts. The larger the simulated lattice, the lower the impact of the distorting lattice is on the accuracy of the simulation. Finally, the y axis was bound to $y = 1.5$ as n'_{c-} values linearly decrease above this point. The two optimisation algorithms used to search for the optimum n_c values are the Nelder-Mead Simplex Method and the Differential Evolution Method. The SciPy [41] python module was used for implementing these algorithms. The Nelder-Mead used the hyperparameters as per Table 1 and the Differential Evolution algorithm used the hyperparameters as per Table 2.

Table 1 - Hyperparameters of the Nelder-Mead Optimisation Algorithm

	Hyperparameters
Vertices of the Starting Simplex	(0, 0.1), (1, 0.1), (0.5, 1)
Maximum Iterations	400
Bounds	$0 \leq x \leq 1$ $0.1 \leq y \leq 1.5$

Table 2 - Hyperparameters of the Differential Evolution Optimisation Algorithm

	Hyperparameters
Population Size	15
Population Initialisation Method	"latinhyperube" – maximising coverage of parameter space
Bounds	$0 \leq x \leq 1$ $0.1 \leq y \leq 1.5$
Perform Local minimisation routine on best individual	"True"

D. Additional Work

Besides the work done on the 2D-1D model, key improvements were made to the 3D-3D model as well, which is extensively used by Dr Castles and Dutta. The 3D-3D $\mathbf{R}_n$ model was re-created with Python and the JIT compiler numba [40] which offered significant performance benefits over MATLAB®. Following this, a vectorised matrix operation variant of the model was made. However, given the size of the matrices generated by the 3D-3D model, this caused a severe decrease in maximum simulation sizes *N* and so a looped paradigm was maintained instead. The second major performance improvement was made using the characteristics of the matrix $\mathbf{R}'_n$. Since $\mathbf{R}'_n$ is a symmetric matrix, only one triangular must be calculated to find every value present in the matrix. The loop was reduced to only iterate over this lower triangular, and then the transposition of this matrix was added to the empty upper triangular of the matrix. These optimisations led to a runtime improvement of ~716% for FCC and ~745% for BCC models. In addition to this, the maximum number of meta-atoms simulated was increased by 42% for BCC and 26% for FCC. This variant of the model is used for their current work and will be used for published research.

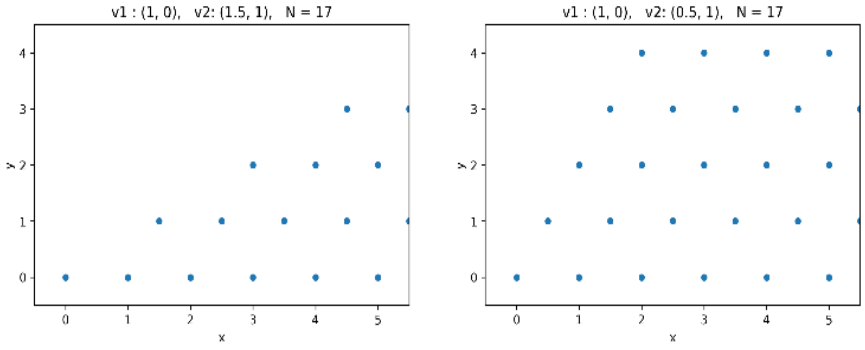

Figure 8 – Visual comparison of the lattices generated by the (0.5,1) and (1.5, 1) vectors.

V. Simulation & Results

Both the Nelder-Mead and Differential Evolution optimisation routines found the same coordinates, up to 4 significant figures, to give the maximum n'_{c-} within the defined parameter space. The optimal values for $\mathbf{v2'}$ are $(0.4924, 0.8703)$, which yield an n'_{c-} of 0.2314. These dimensionless variables roughly correspond to a hexagonal Bravais lattice arrangement. It is important to note that these values were found with an approximated error of 1%.

The Nelder-Mead algorithm made a total of 60 evaluations of the objective function and 31 optimisation iterations, wherein it adjusted the simplex. As can be seen on Fig. 9, the Nelder-Mead did not assess large swaths of the parameter space as a consequence of it being a local optimisation procedure.

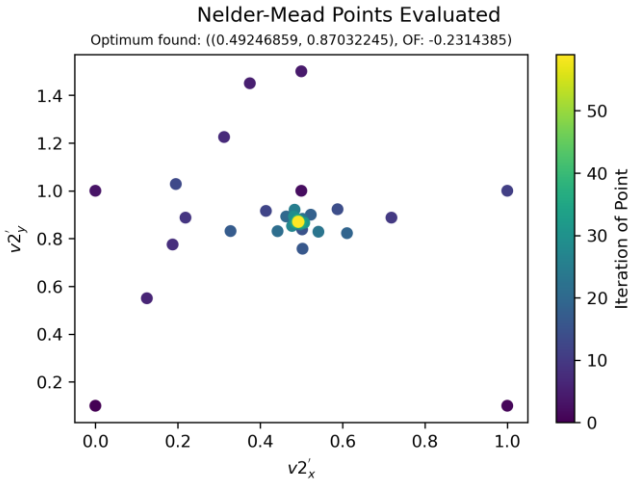

Figure 9 - Visualisation of the Nelder-Mead Algorithm's Evaluations.

The Differential Evolution Algorithm, on the other hand, tests the entire parameter space, as expected of a global optimisation routine. This algorithm made a total of 105 objective function evaluations and preformed a total of 2 optimisation iterations to reach the same conclusion as the Nelder-Mead method.

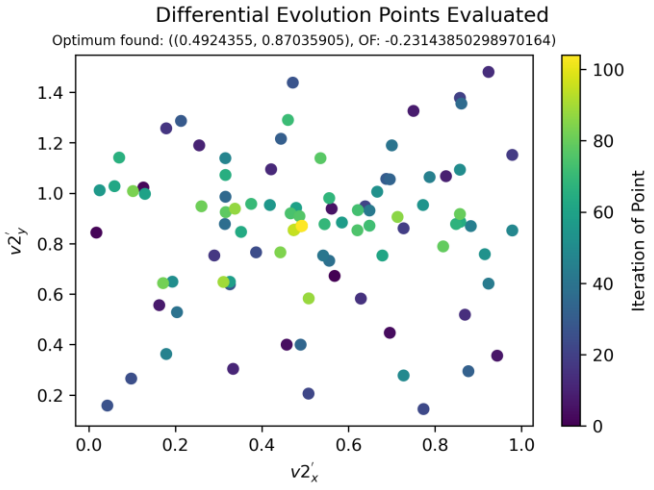

Figure 10 - Visualisation of the Differential Evolution Algorithm's Evaluations.

It is clear that for this type of problem, local optimisation algorithms are preferred as less evaluations lead to the same outcome. Additionally, the correspondence between the results strengthens the case for the hexagonal lattice arrangement being the optimal arrangement for a meta-material consisting of meta-atoms which generate a negative electric susceptibility.

Table 3 - Optimiser Results

	$\mathbf{v2'}$	n'_{c-}
Nelder-Mead	$x' = 0.49239452$ $y' = 0.87033423$	0.23143850293634233
Differential Evolution	$x' = 0.4924355$ $y' = 0.87035905$	0.23143850298970164

VI. Conclusion

Using two optimisation algorithms it was found that the hexagonal lattice structure provides the best compromise between the density and polarisability of meta-atoms in a dimensionless lattice, without spontaneous polarisation occurring. It is therefore recommended for Dr Castles and Dutta to employ a hexagonal lattice geometry in their initial metamaterial prototype, so that they may create the strongest possible "dielectric levitation" effect to experimentally verify the negative electric susceptibility.

VII. Future Work

Additional work can be done in several areas. Firstly, more optimisation algorithms could be tested with this particular setup, and results could be compared. Examples of worthwhile algorithms to test could be Simplicial Homological global optimiser (SHGO) [42]which uses similar principles as the Nelder-Mead, but on a global scale, and a derivate-based method, such as the truncated Newton Algorithm (TNC) [43] to test whether such algorithms may be appropriate for this problem.

Secondly, the current OF evaluations are simulated at a lattice size of 21. This could be done at a higher size to improve the results of the simulation. One way the simulation size could be greatly increased could be via the use of computing clusters, with memory capabilities far greater than the machines used to run the simulations for this report. Additionally, optimisation algorithms such as Differential Evolution lend themselves to parallelisation. Given that such large simulations would be expensive and time consuming, and that clusters are ideal for parallelised tasks, this could also be considered.

Finally, the approaches and lessons learned from this paper could be applied to a 3D-3D model to optimise the crystal structure of a 3D material, rather than a 2D one. More likely than not 3D variants of the metamaterial will see stronger capabilities for generating fields, and therefore the optimisation of that structure could be a worthwhile pursuit. Since the 3D computations are more computationally expensive, and have a larger set of decision variables, a computing cluster and parallelised optimisation algorithms would be heavily reccomended for such a task.

VIII. References

[1] A. Cremonesi *et al.*, "MATERIALS 2030 MANIFESTO Systemic Approach of Advanced Materials for Prosperity – A 2030 Perspective," Feb. 2022.

[2] F. Castles, J. A. J. Fells, D. Isakov, S. M. Morris, A. A. R. Watt, and P. S. Grant, "Active Metamaterials with Negative Static Electric Susceptibility," *Advanced Materials*, vol. 32, no. 9, p. 1904863, Mar. 2020, doi: 10.1002/adma.201904863.

[3] T. M. Sanders, "On the sign of the static susceptibility," *American Journal of Physics*, vol. 56, no. 5, pp. 448–451, May 1988, doi: 10.1119/1.15754.

[4] Q. Gao *et al.*, "Magnetic levitation using diamagnetism: Mechanism, applications and prospects," *Science China Technological Sciences*, vol. 64, no. 1, pp. 44–58, Jan. 2021, doi: 10.1007/s11431-020-1550-1.

[5] C. Kittel, *Introduction to Solid State Physics*, no. 6. 1967. doi: 10.1119/1.1974177.

[6] D. Dugdale, *Essentials of electromagnetism*. London: Macmillan Education UK, 1993. doi: 10.1007/978-1-349-22780-8.

[7] K. M. Rabe and C. H. Ahn, *Physics of Ferroelectrics*, vol. 105. Berlin, Heidelberg: Springer Berlin Heidelberg, 2007. doi: 10.1007/978-3-540-34591-6.

[8] A. R. von Hippel, *Dielectrics and Waves*, 1st ed. Wiley, 1954.

[9] P. Atkins and J. de Paula, *Atkins' physical chemistry*, 10th ed. 2010.

[10] M. D. Simon and A. K. Geim, "Diamagnetic levitation: Flying frogs and floating magnets (invited)," *Journal of Applied Physics*, vol. 87, no. 9, pp. 6200–6204, May 2000, doi: 10.1063/1.372654.

[11] P. B. Allen, "Dipole interactions and electrical polarity in nanosystems: The Clausius–Mossotti and related models," *The Journal of Chemical Physics*, vol. 120, no. 6, pp. 2951–2962, Feb. 2004, doi: 10.1063/1.1630029.

[12] D. E. Aspnes, "Local-field effects and effective-medium theory: A microscopic perspective," *American Journal of Physics*, vol. 50, no. 8, pp. 704–709, Aug. 1982, doi: 10.1119/1.12734.

[13] Y. Liu and X. Zhang, "Metamaterials: a new frontier of science and technology," *Chemical Society Reviews*, vol. 40, no. 5, p. 2494, 2011, doi: 10.1039/c0cs00184h.

[14] S. Xiao, T. Wang, T. Liu, C. Zhou, X. Jiang, and J. Zhang, "Active metamaterials and metadevices: a review," *Journal of Physics D: Applied Physics*, vol. 53, no. 50, p. 503002, Dec. 2020, doi: 10.1088/1361-6463/abaced.

[15] J. Qi *et al.*, "Recent Progress in Active Mechanical Metamaterials and Construction Principles," *Advanced Science*, vol. 9, no. 1, p. 2102662, Jan. 2022, doi: 10.1002/advs.202102662.

[16] "On the rotation of plane of polarisation of electric wave by a twisted structure," *Proceedings of the Royal Society of London*, vol. 63, no. 389–400, pp. 146–152, Dec. 1898, doi: 10.1098/rspl.1898.0019.

[17] V. G. Veselago, "The Electrodynamics Of Substances With Simultaneously Negative Values Of Epsilon And μ," *Soviet Physics Uspekhi*, vol. 10, no. 4, pp. 509–514, Apr. 1968, doi: 10.1070/PU1968v010n04ABEH003699.

[18] J. B. Pendry, A. J. Holden, W. J. Stewart, and I. Youngs, "Extremely Low Frequency Plasmons in Metallic Mesostructures," *Physical Review Letters*, vol. 76, no. 25, pp. 4773–4776, Jun. 1996, doi: 10.1103/PhysRevLett.76.4773.

[19] J. B. Pendry, A. J. Holden, D. J. Robbins, and W. J. Stewart, "Magnetism from conductors and enhanced nonlinear phenomena," *IEEE Transactions on Microwave Theory and Techniques*, vol. 47, no. 11, pp. 2075–2084, 1999, doi: 10.1109/22.798002.

[20] L. Ai and X.-L. Gao, "Metamaterials with negative Poisson's ratio and non-positive thermal expansion," *Composite Structures*, vol. 162, pp. 70–84, Feb. 2017, doi: 10.1016/j.compstruct.2016.11.056.

[21] D. R. Smith, J. B. Pendry, and M. C. K. Wiltshire, "Metamaterials and Negative Refractive Index," *Science (1979)*, vol. 305, no. 5685, pp. 788–792, Aug. 2004, doi: 10.1126/science.1096796.

[22] N. Seddon and T. Bearpark, "Observation of the Inverse Doppler Effect," *Science (1979)*, vol. 302, no. 5650, pp. 1537–1540, Nov. 2003, doi: 10.1126/science.1089342.

[23] Z.-Q. Lu, L. Zhao, H. Ding, and L.-Q. Chen, "A dual-functional metamaterial for integrated vibration isolation and energy harvesting," *Journal of Sound and Vibration*, vol. 509, p. 116251, Sep. 2021, doi: 10.1016/j.jsv.2021.116251.

[24] P. Yu *et al.*, "Broadband Metamaterial Absorbers," *Advanced Optical Materials*, vol. 7, no. 3, p. 1800995, Feb. 2019, doi: 10.1002/adom.201800995.

[25] Y. Yuan *et al.*, "A Scalable Nickel–Cellulose Hybrid Metamaterial with Broadband Light Absorption for Efficient Solar Distillation," *Advanced Materials*, vol. 32, no. 17, p. 1907975, Apr. 2020, doi: 10.1002/adma.201907975.

[26] L. D. Landau, L. P. Pitaevskii, and E. M. Lifshitz, *Electrodynamics of Continuous Media*. Butterworth-Heinemann, 1984.

[27] B. Wood and J. B. Pendry, "Metamaterials at zero frequency," *Journal of Physics: Condensed Matter*, vol. 19, no. 7, p. 076208, Feb. 2007, doi: 10.1088/0953-8984/19/7/076208.

[28] R. Y. Chiao and J. Boyce, "Superluminality, Parelectricity, and Earnshaw's Theorem in Media with Inverted Populations," *Physical Review Letters*, vol. 73, no. 25, pp. 3383–3386, Dec. 1994, doi: 10.1103/PhysRevLett.73.3383.

[29] R. Y. Chiao, E. Bolda, J. Bowie, J. Boyce, J. C. Garrison, and M. W. Mitchell, "Superluminal and parelectric effects in rubidium vapour and ammonia gas," *Quantum and Semiclassical Optics: Journal of the European Optical Society Part B*, vol. 7, no. 3, pp. 279–295, Jun. 1995, doi: 10.1088/1355-5111/7/3/007.

[30] R. Y. Chiao, J. Boyce, and M. W. Mitchell, "Superluminality and parelectricity: The ammonia maser revisited," *Applied Physics B Laser and*

Optics, vol. 60, no. 2–3, pp. 259–265, 1995, doi: 10.1007/BF01135871.

[31] R. Y. Chiao, E. L. Bolda, J. Bowie, J. Boyce, and M. W. Mitchell, "Superluminality and amplifiers," *Progress in Crystal Growth and Characterization of Materials*, vol. 33, no. 1–3, pp. 319–325, 1996, doi: 10.1016/0960-8974(96)83663-1.

[32] J. Jumper *et al.*, "Highly accurate protein structure prediction with AlphaFold," *Nature*, vol. 596, no. 7873, pp. 583–589, Aug. 2021, doi: 10.1038/s41586-021-03819-2.

[33] J. J. de Pablo *et al.*, "New frontiers for the materials genome initiative," *npj Computational Materials*, vol. 5, no. 1, p. 41, Dec. 2019, doi: 10.1038/s41524-019-0173-4.

[34] S. González Fernández, R. Kubus, and J. Mascareñas Pérez-Iñigo, "Innovation Ecosystems in the EU: Policy Evolution and Horizon Europe Proposal Case Study (the Actors' Perspective)," *Sustainability*, vol. 11, no. 17, p. 4735, Aug. 2019, doi: 10.3390/su11174735.

[35] E. K. P. Chong and S. H. Zak, *An Introduction to Optimization*, 4th ed. Wiley, 2013.

[36] R. Horst and H. Tuy, *Global Optimization: Deterministic Approaches* , 3rd ed. Springer, 2010.

[37] M. J. Kochenderfer and T. A. Wheeler, *Algorithms for Optimization* . MIT, 2019.

[38] J. A. Nelder and R. Mead, "A Simplex Method for Function Minimization," *The Computer Journal*, vol. 7, no. 4, pp. 308–313, Jan. 1965, doi: 10.1093/comjnl/7.4.308.

[39] R. Storn and K. Price, "Differential Evolution – A Simple and Efficient Heuristic for global Optimization over Continuous Spaces," *Journal of Global Optimization*, vol. 11, no. 4, pp. 341–359, 1997, doi: 10.1023/A:1008202821328.

[40] S. K. Lam, A. Pitrou, and S. Seibert, "Numba," in *Proceedings of the Second Workshop on the LLVM Compiler Infrastructure in HPC - LLVM '15*, 2015, pp. 1–6. doi: 10.1145/2833157.2833162.

[41] P. Virtanen *et al.*, "SciPy 1.0: fundamental algorithms for scientific computing in Python," *Nature Methods*, vol. 17, no. 3, pp. 261–272, Mar. 2020, doi: 10.1038/s41592-019-0686-2.

[42] S. C. Endres, C. Sandrock, and W. W. Focke, "A simplicial homology algorithm for Lipschitz optimisation," *Journal of Global Optimization*, vol. 72, no. 2, pp. 181–217, Oct. 2018, doi: 10.1007/s10898-018-0645-y.

[43] S. G. Nash, "Newton-Type Minimization Via the Lanczos Method," *SIAM Journal on Numerical Analysis*, vol. 21, no. 4, Aug. 1984.